Organic & Biomolecular Chemistry

ROYAL SOCIETY OF CHEMISTRY

PAPER

View Article Online
View Journal | View Issue

Cite this: *Org. Biomol. Chem.*, 2023, **21**, 4620

Stereoselective oxidation of phenoxathiin-based thiacalix[4]arenes – stereomutation of sulfoxide groups†

N. Broftová,[a] T. Landovský,[a] H. Dvořáková,[b] V. Eigner,[c] M. Krupička[a] and P. Lhoták *[a]

Received 12th May 2023,
Accepted 15th May 2023

DOI: 10.1039/d3ob00530e

rsc.li/obc

A phenoxathiin-based macrocycle represents an inherently chiral building block, well accessible in two steps from the starting thiacalix[4]arene. The oxidized derivatives bearing one sulfoxide group and three sulfonyl groups were found to exhibit unexpected stereochemical preferences of the sulfoxide group during transformations. The sulfoxide moiety is always pointing out of the cavity (S=O *out*), while the opposite (S=O *in*) configuration was never obtained by direct oxidation. In order to achieve full oxidation to sulfone, the configuration of the sulfoxide group must first be changed by a photochemical inversion before the final oxidation occurs. The phenomenon of stereomutation of the sulfoxide group in the thiacalixarene series was studied using a combination of experimental (NMR and single crystal X-ray analysis) and theoretical (DFT) approaches.

Introduction

After their discovery more than two decades ago,[1] thiacalixarenes quickly became an integral part of the calixarene family.[2] The introduction of sulfur instead of classical methylene bridges makes these macrocycles very interesting for various applications in supramolecular chemistry. On the one hand, these derivatives retain some typical properties of classical calixarenes, such as the existence of four basic conformations/atropisomers called *cone*, *partial cone*, *1,2-* and *1,3-alternates*.[2] On the other hand, the presence of heteroatoms brings about some new properties that are not possible with the parent systems. Such new features include altered conformational preferences, significantly different complexation properties, and last but not least, new methods of chemical derivatization of the basic skeleton.[3]

Although the formation of spirodienone derivatives[4] has long been known in the classical calixarene series and is used for the synthesis of some unusual derivatisation patterns,[5] the application of this approach to thiacalixarenes led to the discovery of a completely new type of chemistry. As shown in Scheme 1, the starting thiacalix[4]arene **1** can be smoothly transformed into spirodienone **2**,[6] which is under acidic con-

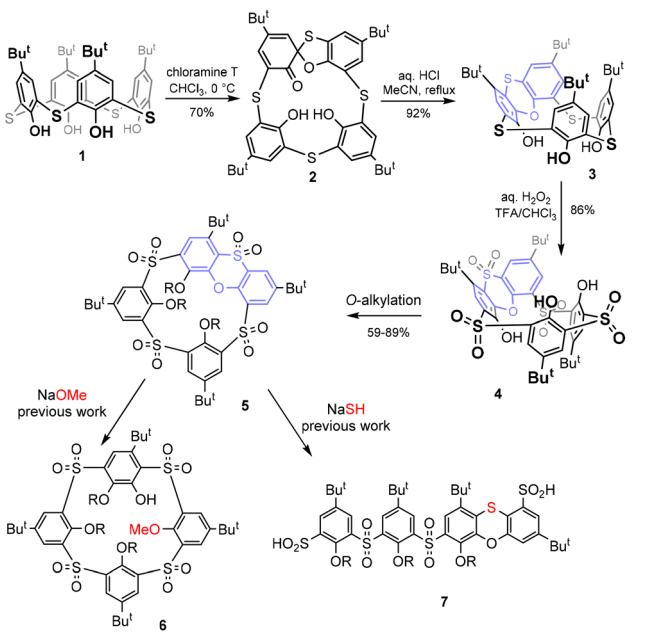

Scheme 1 Synthesis of phenoxathiin-based thiacalixarene and its further transformations.

[a]*Department of Organic Chemistry, University of Chemistry and Technology, Prague (UCTP), Technická 5, 166 28 Prague 6, Czech Republic. E-mail: lhotakp@vscht.cz*
[b]*Laboratory of NMR Spectroscopy, UCTP, Technická 5, 166 28 Prague 6, Czech Republic*
[c]*Department of Solid State Chemistry, UCTP, Technická 5, 166 28 Prague 6, Czech Republic*

†Electronic supplementary information (ESI) available: Spectral characterization of new compounds, temperature-dependent NMR spectra of **12a** and **12b**, and DFT calculations. CCDC 2227440–2227444. For ESI and crystallographic data in CIF or other electronic format see DOI: https://doi.org/10.1039/d3ob00530e

ditions unexpectedly rearranged into phenoxathiin-based macrocycle **3** in a very high yield.[7] Due to the presence of the condensed heterocyclic moiety, compound **3** represents a highly rigidified inherently chiral system with potential application in the design of chiral receptors. During our attempts at the shaping of this skeleton (formation of various conformations) and the oxidation of sulfur bridges, we found[8] that sulfur bridges can be oxidised to yield sulfone **4**, which was alkylated to form intermediate **5**.

Recently, rigid calix[4]arenes[9] with high internal strain have been recognized as surprisingly reactive systems enabling unusual transformations.[10] Similarly, it was found that compound **5** can be used for further unexpected reactions. In the presence of alkoxides, it is subject to a nucleophilic attack[11] leading to a hitherto unexplored type of macrocycle **6**, or it undergoes an unprecedented cascade of nucleophilic cleavage/rearrangements (with SH^-) to form linear oligomers **7** (Scheme 1).[12]

In this paper, we focused on some other interesting aspects of oxidised compound **5** and related systems concerning their unusual stereochemical preferences during the oxidation of sulfur bridges. We hope that a better understanding of this phenomenon can be used in further derivatization of these systems and contribute to the application of these compounds in supramolecular chemistry.

Results and discussion

Thiacalixarene **1** was oxidized using the known procedure[7b] (chloramine T/$CHCl_3$-MeOH) to obtain the corresponding spirodienone derivatives **2** in 74% yield (Scheme 1). The acid-catalysed rearrangement then led to the isolation of **3** in 92% yield. During the oxidation of **3** using the literature conditions (excess of 30% aq. H_2O_2 in TFA/$CHCl_3$),[8] we noticed that the outcome of the reaction can vary from case to case. The careful inspection of the reaction conditions revealed that the ratio of products **4** and **8** depends not only on the reaction time and temperature (as already observed) but is also unexpectedly dependent on the presence or absence of light. Indeed, the reaction carried out at rt in the dark (flask wrapped with aluminum foil) gave compound **8** as the only product in 98% yield (Scheme 2). On the other hand, the same reaction conditions under light led to a mixture of both compounds **4** and **8**. Increasing the temperature (reflux) and prolonging the reaction time (3 days) finally led to the isolation of compound **4** in 86% yield. Interestingly, an attempt at further oxidation of **8** with fresh oxidation agents (in the dark) did not lead to any reaction while the same reaction under light provided **4** in a good yield.

Based on the above results, we can therefore postulate the following unexpected assumption: for the oxidation of the sulfoxide group in compound **8**, a change of the configuration to the opposite stereoisomer is first required, and only then can the oxidation occur by itself (Scheme 2).

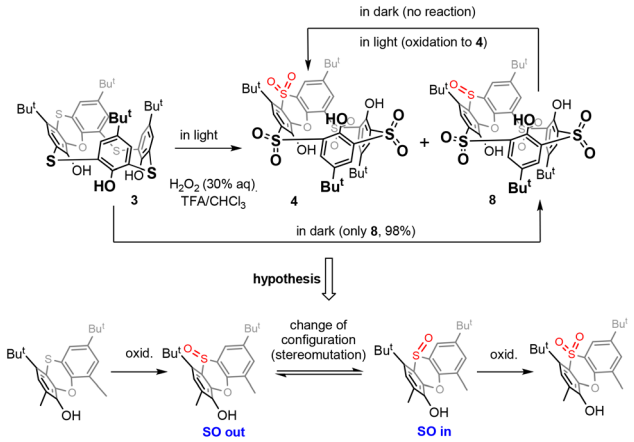

Scheme 2 Oxidation of phenoxathiin-based thiacalixarenes.

The stereochemistry of the sulfoxide group in compound **8** was already assigned by single crystal X-ray measurement[8] which revealed its "out of cavity" configuration (Scheme 2). The fact that the reaction stopped spontaneously at the 3 × SO_2, 1 × SO stage (compound **8**) indicates that the access of the oxidizing agent from inside the cavity is greatly disadvantaged. Even to such an extent that a change in configuration is required first for oxidation (to compound **4**) to occur at all.

This is reminiscent of our earlier observation[13] that the oxidation of sulfur to sulfoxide in thiacalix[4]arenes in the *cone* conformation always occurs on the side opposite to the lower rim of calixarene.[14] In other words, the oxidizing agent always approaches from the side of the upper rim, which is probably sterically more accessible (Fig. 1). In this case, however, the selectivity is not so pronounced and after the oxidation of all bridges to sulfoxide, further oxidation to sulfone normally follows.

Since the non-alkylated derivatives **4** and **8** are difficult to handle (they form long tails in thin-layer chromatography), we decided to study the last oxidation step on alkylated derivatives, which are easily chromatographically separable. Compound **8** was alkylated using an excess of Cs_2CO_3 as a base and alkyl iodide (MeI, EtI, and PrI) as an alkylating agent

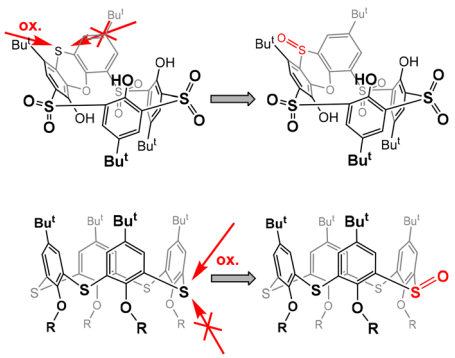

Fig. 1 Preferred approaches for the oxidizing agent during oxidation to sulfoxide.

in acetone. The corresponding peralkylated compounds **9a–c** were isolated in good yields (Scheme 3).

In order to study the possible photochemical stereomutation[15] of the sulfoxide moiety, we first chose an appropriate wavelength of light. The UV/vis spectrum of the starting sulfoxide **9a** in $CHCl_3$ (see the ESI Fig. 43†) showed two maxima at 295 nm (ε_{295} = 9.02 × 10^3 l mol^{-1} cm^{-1}) and 328 nm (ε_{328} = 7.77 × 10^3 l mol^{-1} cm^{-1}), and the maxima for **9b** and **9c** were almost identical (ESI Fig. 44 and 45†). The sample of **9a** was irradiated with light (commercially available LED with a maximum at a wavelength of 311 nm, which was close to the measured maximum of the compound). The reaction was carried out at room temperature and quenched after one day of irradiation. However, we found that under these conditions, the molecule was degraded to some unidentified products and the expected thiacalixarene derivatives were not found in the reaction mixture.[16]

To avoid harsh conditions, we used light with a maximum at 365 nm (commercially available LED). After 24 h, derivative **10a** was isolated from the reaction mixture in 40% yield, together with 31% of the unreacted starting material **9a** (Scheme 3). A similar reaction of **9b** gave product **10b** with the opposite configuration in 58% yield (11% of **9b** was isolated), while a propoxy derivative provided **10c** in 66% yield (14% of **9c** was isolated).

The structure of **10a** was confirmed by HRMS ESI^+ analysis, which showed a peak at *m*/*z* = 895.2283, which was in very good agreement with the value of the $[M + Na]^+$ cation (895.2285) predicted for **10a**. The number of peaks and the splitting patterns of the ^1H NMR spectrum ($CDCl_3$, 400 MHz, 298 K) of **10a** are the same as those of the starting compound. However, some differences are clearly visible here, such as the shift of the singlet of the MeO group from 3.55 (**9a**) to 3.17 (**10a**) or the change in the chemical shift of the *tert*-Bu group from 0.73 (**9a**) to 0.97 (**10a**). In both cases, these are groups that come into close proximity to the S═O function facing the cavity of compound **10a**.

The unequivocal evidence of the inversion of sulfoxide stereochemistry was obtained by single crystal X-ray analysis. Slow crystallization from a $CHCl_3$–EtOH mixture provided **10a** as a solvate with ethanol in the *partial cone* conformation (monoclinic system, space group $P2_1/c$). As shown in Fig. 2a, the sulfur atom of the phenoxathiin system is tilted into the cavity, and the sulfoxide group points toward the neighbouring Bu^t and MeO groups (see above for changes in the NMR spectrum). The inversion of configuration is best highlighted by a comparison with the starting compound **9a** (Fig. 2b). At the same time, the sulfoxide group is responsible for trapping ethanol, which is bound through a hydrogen bond (S═O···H–O = 1.977 Å).

Compound **10b** crystallized in a triclinic system, space group $P\bar{1}$, adopting the *partial cone* conformation. The solvent molecule (CH_3OH) is held by HB interactions with the sulfoxide group (S═O···H–O = 2.051 Å), resembling thus the solvate of **10a** (Fig. 2c). The arrangement is further stabilised by intramolecular close contacts between the sulfonyl oxygen atoms and the ether oxygen atoms of the calixarene skeleton (3.034 Å, 2.861 Å and 3.024 Å). These distances are shorter than the corresponding sum of the van der Waals radii (*ca.*3.04 Å),[17] indicating attractive interactions between the oxygen atoms which can be classified as chalcogen bonding.[18] The same features can be also found within the above **10a**·EtOH complex. Compared to Me or Et derivatives, the introduction of propyl

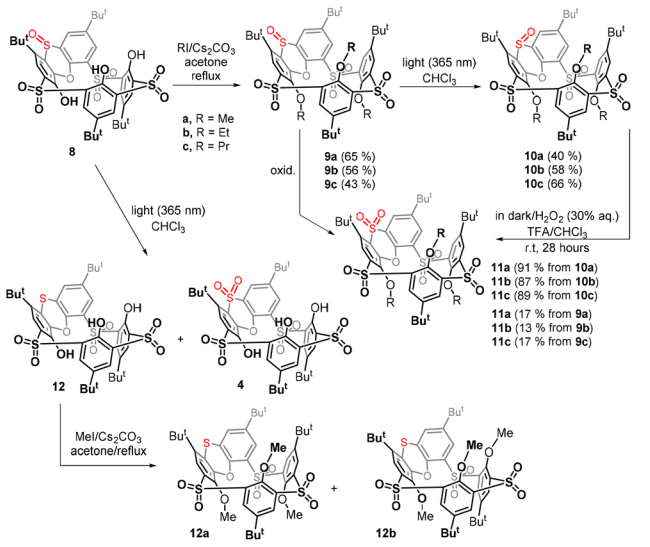

Scheme 3 Stereomutation of the sulfoxide group in phenoxathiin-based thiacalixarenes and subsequent oxidation.

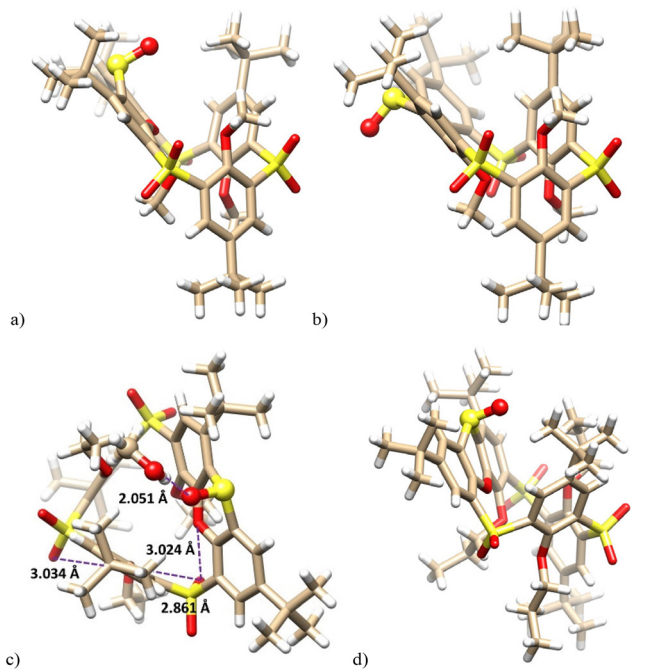

Fig. 2 X-ray structure of: (a) **10a** – side view (EtOH not shown for better clarity); (b) the starting **9a** – side view (ref. 8*a*); (c) **10b** – side view; (d) **10c** – side view, (sulfoxide group shown as balls).

groups had only a minimal effect on the basic geometrical parameters of the system; see the structure of **10c** (Fig. 2d).

Having in hand the corresponding stereoisomers **9a–c** and **10a–c** possessing the *out* and *in* configuration of the sulfoxide group, we were interested in how their subsequent oxidation would proceed. The oxidation of **9a** to tetrasulfone **11a** carried out in the dark under the standard conditions (30% aq. H_2O_2/TFA/$CHCl_3$, room temp) showed only 17% conversion of the starting compound after 28 h. Similar results were also obtained for ethyl and propyl derivatives **9b** and **9c**, where we observed 13% and 17% conversion (^{1}H NMR), respectively (Scheme 3).

In sharp contrast, oxidations of derivatives **10a–c** with the reversed configuration proceeded smoothly in all cases with 100% conversion, and the respective sulfones **11a–c** were isolated by preparative TLC in 91%, 87%, and 89% yields, respectively. The above result confirms our assumptions that the oxidation of the "*in*" configuration is much easier than that of the "*out*" configuration.

In order to confirm these conclusions also for non-alkylated derivatives, compound **8** was irradiated in the same way (light 365 nm, $CHCl_3$, rt) as was done for compounds **9a–c** to achieve the stereomutation of the sulfoxide group.

In addition to the unreacted starting compound **8**, the crude reaction mixture showed the formation of a small amount of sulfone **4**, identified by a comparison of the NMR signals with an authentic sample, while the main product **12** remained unknown (Scheme 3). Since the chromatographic separation of non-alkylated derivatives is very difficult, both products were converted by a reaction with methyl iodide (MeI, K_2CO_3/acetone/reflux) to the corresponding methoxy derivatives and then separated by preparative TLC on silica gel. The formation of sulfone **4** was confirmed by its alkylated product **11a**. Interestingly, the alkylation of **12** led to a mixture of two products **12a** and **12b** possessing the same molecular mass but different ^{1}H NMR spectra, which indicated the formation of two different conformers. Surprisingly, the HRMS ESI$^+$ analysis of the methoxy derivative **12a** showed a molecular peak at m/z = 879.2335, which was in perfect agreement with the $[M + Na]^+$ cation (879.2336) predicted for a compound lacking one oxygen atom. Thus, the main product is not sulfoxide with altered stereochemistry, but compounds **12a** and **12b** possessing a sulfide bridge.

While methylation of tetrasulfone **4** or trisulfone monosulfoxide **8** leads to a single conformation (*partial cone*), the formation of two conformers **12a** and **12b** suggests that the conformational preferences of the sulfur-bridged derivative **12** are significantly altered. To reveal the possible mobility of alkylated derivatives **12a** and **12b**, the VT ^{1}H NMR studies of both products were carried out. While heating of **12a** (500 MHz, $CDCl_2$–$CDCl_2$) did not lead to any change of the spectrum (see the ESI†), compound **12b** assigned as the *1,2-alternate* was gradually transformed into **12a** at 110 °C (see Fig. 4). This suggests that (i) the sulfur bridge in **12** presents less steric hindrance than sulfone **4** or sulfoxide **8**, where a similar change is not possible; (ii) the *partial cone* conformer **12a** represents a thermodynamically more stable conformation than **12b**. This was further confirmed by heating a solution of compound **12b** in $CDCl_2$–$CDCl_2$ overnight at 120 °C, which led to complete conversion to compound **12a**.

The final proof of the structure was obtained by the single crystal X-ray analysis of **12a**. This revealed that compound **12a** crystallized as a solvate with cyclohexane (**12a**·C_6H_{12}) in a monoclinic system, space group $P2_1/c$. As shown in Fig. 3a, the molecule adopts the *partial cone* conformation and the missing oxygen atom was removed in the phenoxathiin moiety, thus forming a sulfide bridge. The conformation was stabilised by an array of intramolecular close contacts between the oxygen atoms from SO_2 and OR moieties (2.890 Å, 2.883 Å, 2.869 Å and 3.039 Å), which can be classified as chalcogen bonds (Fig. 3b).

The crystal packing of **12a** (Fig. 3c) was characterised by the infinite chains of calixarenes held together by the intermolecular chalcogen bonds between the sulfide S atoms and one of the S═O bonds of the opposite sulfone bridge. An S···O═S distance of 3.186 Å was reasonably shorter than the

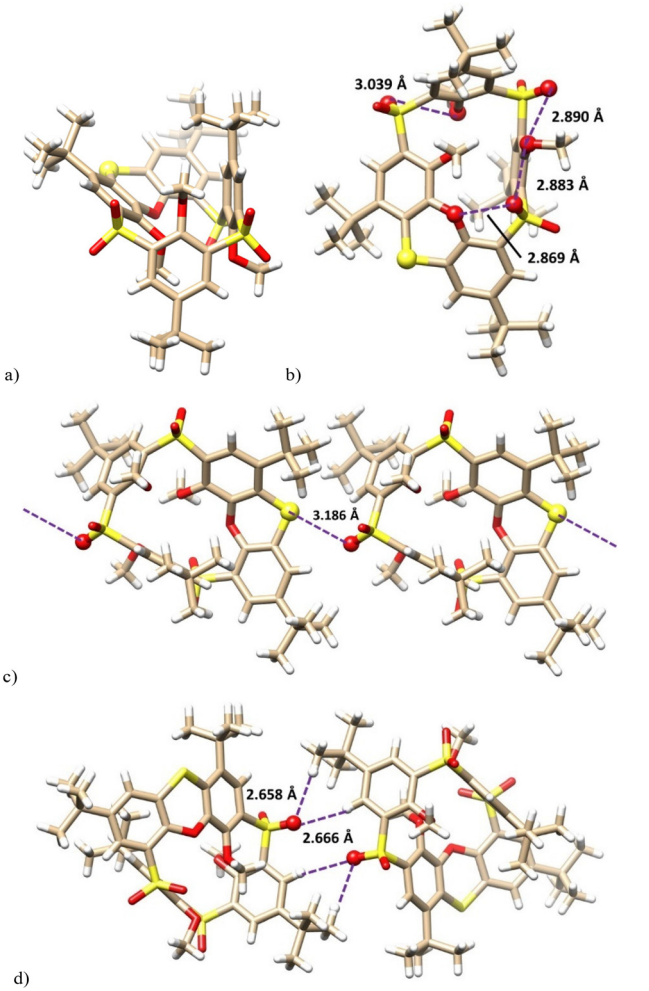

Fig. 3 X-ray structure of: (a) **12a** — side view; (b) **12a** — bottom view of the same indicating the close contacts between the oxygen atoms; (c) the chalcogen bonds in the infinite chain; (d) non-classical hydrogen bonds between the chains.

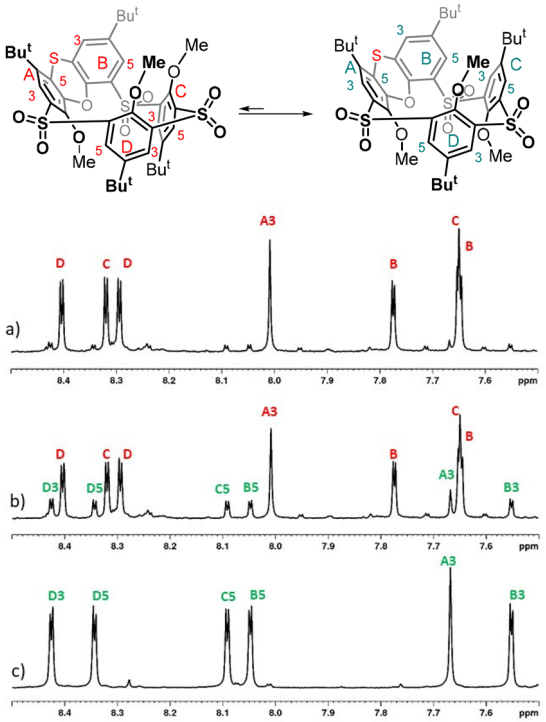

Fig. 4 ^{1}H NMR spectra of: (a) **12b** before heating (sample contained a small amount of isomer **12a** due to non-ideal preparative TLC separation of products; (b) **12b** after heating up to 110 °C (peaks corresponding to **12a** visibly increased); (c) **12a**.

corresponding sum of vdW radii (3.32 Å).[17] The individual chains are interconnected (see Fig. 3d) by non-classical hydrogen bonds between S═O groups and hydrogens in *tert*-butyl groups (S═O···H = 2.658 Å) and on the aromatic subunits (S═O···H_{arom} = 2.666 Å).

The formation of both reduced and oxidised compounds during the attempted stereomutation of **8** was rather unexpected. To avoid possible confusion about the oxygen source for oxidation, the reaction was performed under argon in carefully degassed chloroform, but the result was the same. It indicates that the sulfoxide S═O bond in **8** was cleaved during the reaction, yielding **12**. Such reactions (deoxygenations) are known from the chemistry of aromatic sulfoxides,[19] and the resulting highly reactive oxygen species[20] usually react with the environment (solvent) to form oxidized products. In our case, the only oxidizable molecule in the system (besides chloroform) is the starting sulfoxide **8**, so the formation of a small amount of by-product **4** seems to be a more or less logical consequence.

To further support this idea, we repeated the reaction under identical conditions but with the addition of diphenyl sulfide as the presumed oxygen acceptor. After 11 hours of irradiation (364 nm) and subsequent methylation of the crude reaction mixture with MeI, the ^{1}H NMR analysis showed three calixarene compounds **12a**, **12b** and **9a** in 14%, 7% and 79% yields. The isomers **12a** and **12b** were obtained after column chromatography in 12% and 5% yields.

In any case, compound **12** represents the only example of its kind, where there is an unoxidized sulfur bridge together with the sulfone bridges. To the best of our knowledge, a similar type of compound has not yet been described for thiacalixarenes, because the oxidation of sulfur atoms always proceeds in such a way that sulfones begin to form only after all the sulfur bridges have been oxidized to sulfoxides.

Important parts of the reaction pathway were modelled using DFT. The detailed sequence of the multiple oxidation steps is beyond the scope of this research, hence we assumed that the sulphur bridges are fully oxidized before phenoxathiine oxidation takes place. Conformational screening of all structures was performed using CREST, and 30 lowest-lying conformers were optimized at the B3LYP/def2-SVP level with D3BJ corrections. The energy of the most favourable conformer is reported. The reactivity is expected to be guided by steric repulsion, which is usually well described at the DFT level, but due to a wide range of functional groups present in the molecule, final DLPNO-CCSD(T)/def2-QZVPP single point energy evaluation was performed. The relative energies at the DFT level differ quite substantially from CCSD(T) and both values are reported, with the DFT value (in *italics*).

From the thermodynamic point of view, the structures of **9a** and **10a**, possessing the *out* and *in* configuration of the sulfoxide group are close in energy, with the isomer **9a** (*out*) being preferred by 3.3 (*0.5*) kcal mol^{-1}. The reaction energy of the second oxidation step from sulfoxide **9a** to sulfone **11a** is −68 (*−51*) kcal mol^{-1}, significantly more favoured than the first step, sulfide **12a** to sulfoxide (**9a** or **10a**), which is −41 (*−28*) kcal mol^{-1}.

The kinetics of the oxidation steps was examined with respect to the approach of the oxidant, modelled using trifluoroperoxoacetic acid (TFPA). Both transition states leading to **9a** and **10a** were found, and the attack from *outside* was preferred by about 2.1 (*−1.7*) kcal mol^{-1}. The second oxidation step, from sulfoxide to sulfone, proceeds from above the molecule, rather across the calixarene ring. The activation energy of the oxidation of **9a** is 1.1 (*−0.3*) kcal mol^{-1} higher than that of the **10a** isomer. The whole reaction sequence is shown in Fig. 5.

The difference in activation energy for the isomers agrees with the experimental results of the first oxidation step. In the second step, the calculated energy difference favors the oxidation of **10a**, with S═O pointing inwards, which is impossible without the isomerization of sulfoxide. The intuitive explanation using the argument of the steric hindrance of the calixarene ring is probably justified in this case. In addition, the extent of HOMO delocalization to aromatic rings is smaller in **10a**, making the lone pair on sulphur more reactive in the S═O *in* isomer.

The insufficiency of a computational model may come into play. Nevertheless, steric interactions are usually well described at the applied DFT-D3 level of theory, providing good geometries of intermediates and transition states. The role of solvent is not expected to be very important, namely, when comparing two very similar stereoisomers. The steric effects are presumably not the only contribution, for example

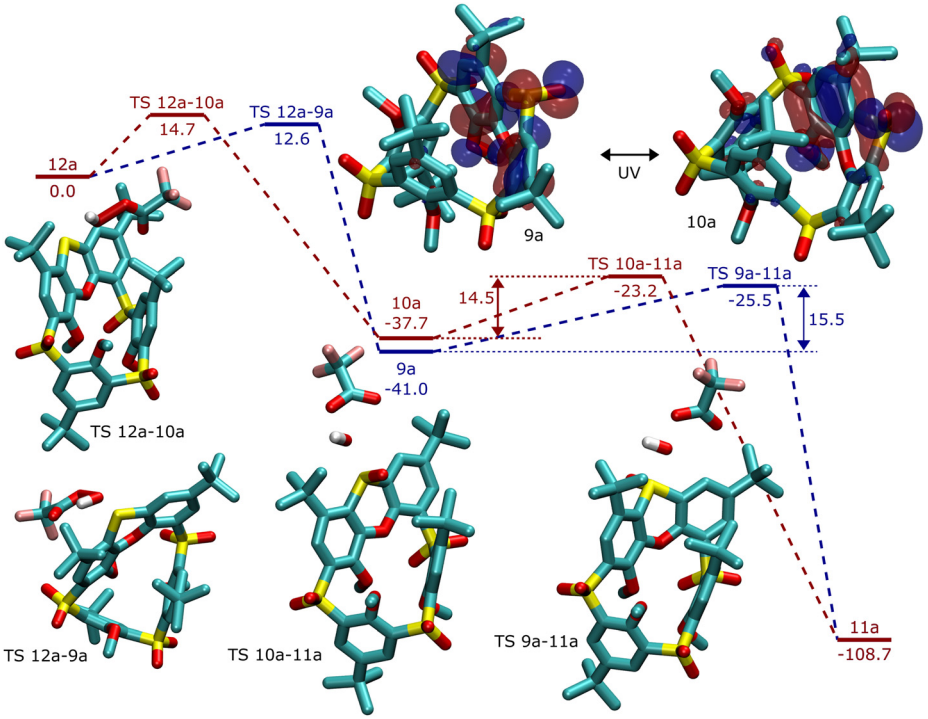

Fig. 5 Reaction profile for stepwise oxidation of sulfide **12a** to sulfone **11a** through two different (*in–out*) sulfoxides, **9a** and **10a**. Relative energies were calculated at the CCSD(T) level. In the insets, the structures of transition states are shown, together with the HOMO orbitals (at the DFT level) of sulfoxides **9a** and **10a**.

in Fig. 5, phenoxathiin-oxide is deformed *inwards* during the oxidation of **10a**, contributing to the increased activation energy.

Conclusion

Phenoxathiin-based thiacalixarene is well accessible in two steps starting from thiacalix[4]arene and represents an inherently chiral building block. The oxidised forms of this macrocycle bearing 3 sulfonyl and 1 sulfoxide groups were found to exhibit unexpected stereochemical preferences during its transformation to a fully oxidised macrocycle ($4 \times SO_2$). The sulfoxide group, which is part of the phenoxathiin moiety, is always pointing out of the cavity (S═O *out*), while the opposite (S═O *in*) configuration has never been obtained by direct oxidation. In order to achieve full oxidation, the configuration of the sulfoxide group must first be changed by a photochemical reaction before the final oxidation step occurs. The phenomenon of stereomutation of the sulfoxide group in this thiacalix[4]arene series was studied using a combination of experimental (NMR and single crystal X-ray analysis) and theoretical (DFT) approaches.

Experimental section

General experimental procedures

All chemicals were purchased from commercial sources and were used without further purification. Acetone was dried and distilled using conventional methods and acetonitrile was dried using a column solvent purification system, PureSolv MD7 (Inert). All samples were dried in a desiccator over P_2O_5 under vacuum (1 Torr) for 8 hours. Melting points were measured on Heiztisch Mikroskop Polytherm A (Wagner & Munz) and they were not corrected. ^{1}H, ^{13}C, COSY, HMQC and HMBC, and NOE spectra were measured on Bruker Avance^{III} 600 operating at 600.13 MHz for ^{1}H and 150.92 MHz for ^{13}C, Bruker Avance III 500 MHz operating at 500.13 MHz for ^{1}H and 125.77 MHz for ^{13}C or Agilent 400-MR DDR2 operating at 400 MHz for ^{1}H. Chemical shifts are given in δ-units (ppm) and were referenced to TMS. IR spectra were measured on a Nicolet 6700 (Thermo-Nicolet) FTIR spectrometer connected with a diamond ATR attachment GladiATR (PIKE) and DTGS detector. The measurement parameters were 4000–400 cm^{-1} spectral range, 4 cm^{-1} resolution, 64 spectral accumulations and Happ-Genzel apodization. ESI HRMS spectra were measured on a Q-TOF (Micromass) spectrometer. UV-Vis spectra were acquired on a dual beam UV-Vis spectrophotometer Varian CARY 50 CONC (Varian). UV spectra were recorded in the range of 200–800 nm with a step of 4 nm. The sample concentration was 1×10^{-3} mol L^{-1}. The purity of the substances and courses of the reactions were monitored by thin layer chromatography (TLC) using silica gel 60 F_{254} on aluminum-backed sheets (Merck) and analyzed at 254 and 365 nm. Column chromatography was performed on silica gel 60 with a particle size of 0.063–0.200 mm (Merck). Radial chromatography was carried out on Chromatotron (Harrison

Research) connected with Lab Pump RHSY2 (Fluid Metering). Self-prepared glass discs were covered using silica gel 60 PF_{254} containing $CaSO_4$ (Merck). Preparative TLC was carried out on self-prepared glass plates (25 × 25 cm) covered by silica gel 60 PF_{254} containing $CaSO_4$ (Merck).

Synthetic procedures

Compound 4. Macrocycle **2** (5.20 g, 7.23 mmol) was dissolved in chloroform (70 mL). Trifluoroacetic acid (24 mL) and hydrogen peroxide (30% aq. sol., 79 mL) were added and the solution was refluxed (62 °C) for 4 days. After 4 days, the solution was stirred and exposed to light (365 nm) for 3 days at room temperature and finally refluxed for another 3 days. Subsequently, the reaction mixture was cooled and Na_2SO_3 was slowly added until no oxidation reaction was observable by a potassium iodine starch test. The resulting mixture was extracted with dichloromethane (3 × 50 mL) and the combined organic layers were dried over $MgSO_4$. The solvent was subsequently removed under reduced pressure to yield compound **4** as a racemic mixture with sufficient purity (white solid, 5.14 g, 84%).

Data for **4** were in accordance with the previously published data.[8]

Compound 8. Macrocycle **2** (1 g, 1.39 mmol) was dissolved in chloroform (52 mL) and stirred at room temperature. The flask was wrapped with aluminium film. Trifluoroacetic acid (18 mL) and hydrogen peroxide (30% aq. sol., 57 mL) were added to the solution and stirred overnight. Na_2SO_3 was slowly added until no oxidation reaction was observable by a potassium iodine starch test. The resulting mixture was extracted with dichloromethane (3 × 50 mL) and the combined organic layers were dried over $MgSO_4$. The solvent was subsequently removed under reduced pressure to yield compound **8** as a racemic mixture with sufficient purity (white solid, 1.129 g, 98%).

Data for **8** were in accordance with the previously published data.[8] Compounds **9a–c** were prepared according to the published procedure.[8]

Compound 10a. Macrocycle **9a** was dissolved (279.2 mg, 0.32 mmol) in chloroform (30 mL). The solution was exposed to light (365 nm) for a day. Subsequently, the solvent was removed from the reaction mixture under reduced pressure. Compound **10a** was isolated using column chromatography (eluent ethyl acetate : cyclohexane 1 : 10 v/v) as a racemic mixture (white solid, 111.2 mg, 40%).

*Data for **10a**.* M.p. > 250 °C. ^{1}H NMR (400 MHz, $CDCl_3$, 298 K): 8.52 (d, 1H, Ar–H, J = 2.5 Hz), 8.50 (d, 1H, Ar–H, J = 2.3 Hz), 8.41 (d, 1H, Ar–H, J = 2.5), 8.20 (d, 1H, Ar–H, J = 2.5), 8.15 (d, 1H, Ar–H, J = 2.3 Hz), 7.90 (s, 1H), 7.03 (d, 1H, Ar–H, J = 2.5 Hz), 4.14 (s, 3H, O–CH_3), 3.78 (s, 3H, O–CH_3), 3.17 (s, 3H, O–CH_3), 1.65 (s, 9H, *t*Bu–H), 1.50 (s, 9H, *t*Bu–H), 1.47 (s, 9H, *t*Bu–H), 0.97 (s, 9H, *t*Bu–H). ^{13}C NMR (126 MHz, $CDCl_3$, 298 K): 155.61, 155.34, 148.97, 148.11, 147.38, 147.08, 143.47, 141.69, 140.76, 138.33, 136.71, 136.39, 135.70, 134.49, 132.87, 132.61, 132.01, 131.60, 130.66, 130.57, 130.33, 127.24, 124.55, 118.66, 77.30, 77.04, 76.79, 66.55, 65.35, 63.31, 32.81, 31.24, 31.22, 30.25. IR (ATR) ν (cm^{-1}): 2957, 2870, 1478, 1423, 1316, 1133. HRMS (ESI^+) ($C_{43}H_{52}O_{11}S_4$) m/z calc: 895.2285 $[M + Na]^+$, found: 895.2283 $[M + Na]^+$.

Compound 10b. Macrocycle **9b** was dissolved (203.5 mg, 0.22 mmol) in chloroform (25 mL). The solution was exposed to light (365 nm) for a day. Subsequently, the solvent was removed from the reaction mixture under reduced pressure. Compound **10a** was isolated using column chromatography (eluent ethyl acetate : cyclohexane 1 : 10 v/v) as a racemic mixture (white solid, 117.3 mg, 58%).

*Data for **10b**.* M.p. > 250 °C. ^{1}H NMR (500 MHz, $CDCl_3$, 298 K): 8.45 (d, 1H, Ar–H, J = 2.3 Hz), 8.40 (d, 1H, Ar–H, J = 2.5 Hz), 8.33 (d, 1H, Ar–H, J = 2.5 Hz), 8.12 (d, 1H, Ar–H, J = 2.5 Hz), 8.07 (d, 1H, Ar–H, J = 2.3 Hz), 7.90 (s, 1H, Ar–H), 6.92 (d, 1H, Ar–H, J = 2.4 Hz), 4.41–4.32 (m, 1H, O–CH2), 4.28–4.13 (m, 2H, O–CH2), 4.10–4.01 (m, 1H, O–CH2), 3.95–3.86 (m, 1H, O–CH2), 3.36–3.27 (m, 1H, O–CH2), 1.59 (s, 9H, *t*Bu–H), 1.43 (s, 9H, *t*Bu–H), 1.41 (s, 9H, *t*Bu–H), 1.37 (t, 3H, O–CH_3, J = 6.9 Hz,), 0.92 (s, 9H, *t*Bu–H), 0.82 (t, 3H, O–CH_3, J = 7.0 Hz), 0.48 (t, 3H, O–CH_3, J = 6.9 Hz).^{13}C NMR (126 MHz, $CDCl_3$, 298 K): 154.82, 152.84, 148.76, 147.59, 146.64, 146.41, 144.62, 142.26, 141.04, 137.55, 137.41, 136.36, 135.90, 134.85, 132.28, 132.06, 131.61, 131.26, 131.04, 130.94, 130.42, 127.62, 124.44, 119.49, 77.31, 77.06, 76.80, 76.58, 73.74, 72.29, 37.89, 35.50, 35.44, 34.71, 32.93, 31.29, 31.25, 30.32, 29.73, 15.52, 14.45, 14.26. IR (ATR) ν (cm^{-1}): 2960, 2870, 1456, 1434, 1315, 1133. HRMS (ESI^+) ($C_{46}H_{58}O_{11}S_4$) m/z calc: 937.2754 $[M + Na]^+$, found: 937.2752 $[M + Na]^+$.

Compound 10c. Macrocycle **9c** was dissolved (122.5 mg, 0.13 mmol) in chloroform (15 mL). The solution was exposed to light (365 nm) for a day. Subsequently, the solvent was removed from the reaction mixture under reduced pressure. Compound **10c** was isolated using column chromatography (eluent ethyl acetate : cyclohexane 1 : 10 v/v) as a racemic mixture (white solid, 73.7 mg, 66%).

*Data for **10c**.* M.p. > 250 °C. ^{1}H NMR (400 MHz, $CDCl_3$, 298 K): ^{1}H NMR ($CDCl_3$, 400 MHz, 298 K) δ (ppm): 8.51 (d, 1H, Ar–H, J = 2.3 Hz), 8.45 (d, 1H, Ar–H, J = 2.5 Hz), 8.37 (d, 1H, Ar–H, J = 2.5 Hz), 8.18 (d, 1H, Ar–H, J = 2.5 Hz), 8.12 (d, 1H, Ar–H, J = 2.3 Hz), 7.94 (s, 1H, Ar–H), 7.03 (d, 1H, Ar–H, J = 2.5 Hz), 4.30–4.22 (m, 1H, O–CH2), 4.22–4.17 (m, 1H, O–CH2), 4.17–4.11 (m, 1H, O–CH2), 4.05–3.96 (m, 1H, O–CH2), 3.96–3.87 (, 1H, O–CH2), 3.24–3.13 (m, 1H, O–CH2), 1.97–1.83 (m, 2H, –CH2), 1.63 (s, 9H, *t*Bu–H), 1.47 (s, 9H, *t*Bu–H), 1.46 (s, 9H, *t*Bu–H), 1.39–1.23 (m, 2H, –CH2), 1.21–1.03 (m, 2H, –CH2), 0.99 (t, 3H, –CH_3, J = 7.4 Hz), 0.98 (s, 9H, *t*Bu–H), 0.60 (t, 3H, –CH_3, J = 7.5 Hz), 0.28 (t, 3H, –CH_3, J = 7.5 Hz).^{13}C NMR (126 MHz, $CDCl_3$, 298 K): 155.02, 153.43, 148.70, 147.34, 146.59, 146.06, 144.55, 142.25, 140.97, 137.38, 137.37, 136.23, 135.65, 134.85, 132.33, 132.04, 131.76, 131.52, 131.51, 131.06, 130.25, 127.60, 124.42, 119.55, 82.55, 79.89, 78.14, 77.25, 77.00, 76.74, 37.72, 35.45, 35.35, 34.65, 32.83, 31.21, 31.15, 30.25, 22.97, 22.31, 21.84, 10.09, 9.81, 9.01. HRMS (ESI^+) ($C_{49}H_{64}O_{11}S_4$) m/z calc: 979.3224 $[M + Na]^+$, found: 979.3224 $[M + Na]^+$.

Compound 11a. Macrocycle **10a** (25 mg, 0.029 mmol) was dissolved in chloroform (10 mL) and stirred at room temperature. The flask was wrapped with aluminium film. Trifluoroacetic acid (5 mL) and hydrogen peroxide (30% aq. sol., 10 mL) were added. The solution was stirred at room temperature for 28 h. Na_2SO_3 was slowly added until no oxidation reaction was observable by a potassium iodine starch test. The mixture was extracted with dichloromethane (5 × 10 mL) and the combined organic layers were dried over $MgSO_4$. The solvent was subsequently removed under reduced pressure. Compound **11a** was isolated using column chromatography (eluent ethyl acetate : cyclohexane 1 : 10 v/v) as a racemic mixture (white solid, 23.2 mg, 91%).

Data for **11a** were in accordance with the previously published data.[8]

Compound **11a** was obtained in 17% yield under identical reaction conditions using derivative **9a** as the starting compound.

Compound 11b. Macrocycle **10b** (25 mg, 0.027 mmol) was dissolved in chloroform (10 mL) and stirred at room temperature. The flask was wrapped with aluminium film. Trifluoroacetic acid (5 mL) and hydrogen peroxide (30% aq. sol., 10 mL) were added. The solution was stirred at room temperature for 28 h and Na_2SO_3 was slowly added until no oxidation reaction was observable by a potassium iodine starch test. The mixture was extracted with dichloromethane (5 × 10 mL) and the combined organic layers were dried over $MgSO_4$. The solvent was subsequently removed under reduced pressure. Compound **11b** was isolated using column chromatography (eluent ethyl acetate : cyclohexane 1 : 10 v/v) as a racemic mixture (white solid, 22.6 mg, 89%).

Data for **11b** were in accordance with the previously published data.[8]

Compound **11b** was obtained in 13% yield under identical reaction conditions using derivative **9b** as the starting compound.

Compound 11c. Macrocycle **10c** (25 mg, 0.026 mmol) was dissolved in chloroform (10 mL) and stirred at room temperature. The flask was wrapped with aluminium film. Trifluoroacetic acid (5 mL) and hydrogen peroxide (30% aq. sol., 10 mL) were added. The solution was stirred at room temperature for 28 h and Na_2SO_3 was slowly added until no oxidation reaction was observable by a potassium iodine starch test. The mixture was extracted with dichloromethane (5 × 10 mL) and the combined organic layers were dried over $MgSO_4$. The solvent was subsequently removed under reduced pressure. Compound **11c** was isolated using column chromatography (eluent ethyl acetate : cyclohexane 1 : 10 v/v) as a racemic mixture (white solid, 22.1 mg, 87%).

Data for **11c** were in accordance with the previously published data.[8]

Compound **11c** was obtained in 17% yield under identical reaction conditions using derivative **9c** as the starting compound.

Compound 11a. Macrocycle **9a** (25 mg, 0.029 mmol) was dissolved in chloroform (10 mL) and stirred at room temperature. The flask was wrapped with aluminium film. Trifluoroacetic acid (5 mL) and hydrogen peroxide (30% aq. sol., 10 mL) were added. The solution was stirred at room temperature for 28 h and Na_2SO_3 was slowly added until no oxidation reaction was observable by a potassium iodine starch test. The mixture was extracted with dichloromethane (5 × 10 mL) and the combined organic layers were dried over $MgSO_4$. The solvent was subsequently removed under reduced pressure. Compound **11a** was isolated using column chromatography (eluent ethyl acetate : cyclohexane 1 : 10 v/v) as a racemic mixture (white solid, 4.3 mg, 17%).

Data for **11a** were in accordance with the previously published data.[8]

Compound 11b. Macrocycle **9b** (25 mg, 0.027 mmol) was dissolved in chloroform (10 mL) and stirred at room temperature. The flask was wrapped with aluminium film. Trifluoroacetic acid (5 mL) and hydrogen peroxide (30% aq. sol., 10 mL) were added. The solution was stirred at room temperature for 28 h and Na_2SO_3 was slowly added until no oxidation reaction was observable by a potassium iodine starch test. The mixture was extracted with dichloromethane (5 × 10 mL) and the combined organic layers were dried over $MgSO_4$. The solvent was subsequently removed under reduced pressure. Compound **11b** was isolated using column chromatography (eluent ethyl acetate : cyclohexane 1 : 10 v/v) as a racemic mixture (white solid, 3.3 mg, 13%).

Data for **11b** were in accordance with the previously published data.[8]

Compound 11c. Macrocycle **9c** (25 mg, 0.026 mmol) was dissolved in chloroform (10 mL) and stirred at room temperature. The flask was wrapped with aluminium film. Trifluoroacetic acid (5 mL) and hydrogen peroxide (30% aq. sol., 10 mL) were added. The solution was stirred at room temperature for 28 h and Na_2SO_3 was slowly added until no oxidation reaction was observable by a potassium iodine starch test. The mixture was extracted with dichloromethane (5 × 10 mL) and the combined organic layers were dried over $MgSO_4$. The solvent was subsequently removed under reduced pressure. Compound **11c** was isolated using column chromatography (eluent ethyl acetate : cyclohexane 1 : 10 v/v) as a racemic mixture (white solid, 4.3 mg, 17%).

Data for **11c** were in accordance with the previously published data.[8]

Compounds 12a and 12b. Macrocycle **8** (100 mg, 0.12 mmol) was dissolved in chloroform (10 mL) under argon and diphenyl sulphide (0.4 mL, 2.4 mmol) was added. The solution was exposed to light (364 nm) for 11 h at room temperature under stirring. Chloroform was then evaporated and the crude reaction mixture was subjected to alkylation.

The residue was suspended in dry acetonitrile (10 mL) and caesium carbonate (800 mg, 2.45 mmol) was added to the mixture. The suspension was stirred for 30 minutes. After that, methyl iodide (0.18 mL, 2.9 mmol) was added and the reaction mixture was heated under reflux overnight. Then, the solvent was removed under reduced pressure. The residue was dissolved in chloroform (10 mL) and water (10 mL). The layers

were separated and the aqueous phase was extracted with chloroform (3 × 20 mL). Combined organic layers were dried over $MgSO_4$. The solvent was evaporated and the residue was purified by silica gel chromatography (eluent ethyl acetate : cyclohexane 1 : 6 v/v) to give compound **12a** (12 mg, 12%) and compound **12b** (5 mg, 5%) as white solids together with 55 mg of compound **11a** (from unreacted **8**).

Compound 12a. ^{1}H NMR (600 MHz, CD_2Cl_2, 298 K): 8.45 (d, 1H, Ar–H–*D3*, *J* = 2.5 Hz), 8.37 (d, 1H, Ar–H–*D5*, *J* = 2.5 Hz), 8.12 (d, 1H, Ar–H–*C5*, *J* = 2.5), 8.08 (d, 1H, Ar–H–*B5*, *J* = 2.3), 7.69 (s, 1H–*A3*), 7.59 (d, 1H, Ar–H–*B3*, *J* = 2.3 Hz), 6.63 (d, 1H, Ar–H–*C3*, *J* = 2.5 Hz), 4.11 (s, 3H, O–CH_3–*C*), 3.84 (s, 3H, O–CH_3–*D*), 3.40 (s, 3H, O–CH_3–*A*), 1.52 (s, 9H, *t*Bu–H–*D*), 1.48 (s, 9H, *t*Bu–H–*A*), 1.44 (s, 9H, *t*Bu–H–*B*), 0.93 (s, 9H, *t*Bu–H–*C*). ^{13}C NMR (150 MHz, CD_2Cl_2, 298 K): 154.88 (quart. C–*C1*), 154.19 (quart. C–*D1*), 148.80 (quart. C–*B4*), 147.98 (quart. C–*D4*), 146.88 (quart. C–*A*), 146.14 (quart. C–*B1*), 145.49 (quart. C–*C4*), 142.67 (quart. C–*A4*), 142.47 (quart. C–*A1*), 137.27 (quart. C–*D6*), 136.02 (quart. C–*C6*), 135.78 (quart. C–*D2*), 135.43 (quart. C–*C2*), 134.62 (quart. C–*A*), 132.43 (CH–*C5*), 132.18 (CH–*D3*), 131.32 (CH–*D5*), 130.91 (CH–*C3*), 129.65 (CH–*B3*), 128.32 (quart. C–*B6*), 127.39 (CH–*B5*), 123.72 (quart. C–*A*), 123.47 (quart. C–*B2*), 118.60 (CH–*A3*), 65.64 (O–CH_3–*C*), 65.15 (O–CH_3–*D*), 61.76 (O–CH_3–*A*), 36.50 (quart. *t*Bu–C–*A*), 35.12 (quart. *t*Bu–C–*D*), 34.95 (quart. *t*Bu–C–*B*), 34.33 (quart. *t*Bu–C–*C*), 30.90 (*t*Bu–C–*B* + *D*), 30.15 (*t*Bu–C–*C*), 29.61 (*t*Bu–C–*A*).

Compound 12b. ^{1}H NMR (600 MHz, CD_2Cl_2, 298 K): 8.42 (d, 1H, Ar–H–*D*, *J* = 2.6 Hz), 8.35 (d, 1H, Ar–H–*C*, *J* = 2.5 Hz), 8.33 (d, 1H, Ar–H–*D*, *J* = 2.6), 8.03 (s, 1H–*A*3), 7.80 (d, 1H, Ar–H–*B*, *J* = 2.3), 7.70 (d, 1H, Ar–H–*C*, *J* = 2.5 Hz), 7.69 (d, 1H, Ar–H–*B*, *J* = 2.3 Hz), 3.77 (s, 3H, O–CH_3–*C*), 3.71 (s, 3H, O–CH_3–*A*), 2.50 (s, 3H, O–CH_3–*D*), 1.63 (s, 9H, *t*Bu–H–*A*), 1.44 (s, 9H, *t*Bu–H–*D*), 1.32 (s, 9H, *t*Bu–H–*B*), 1.30 (s, 9H, *t*Bu–H–*C*). NMR (150 MHz, CD_2Cl_2, 298 K): 155.21 (quart. C), 153.47 (quart. C), 152.58 (quart. C), 150.33 (quart. C), 149.35 (quart. C), 149.28 (quart. C), 148.34 (quart. C), 148.29 (quart), 143.05 (quart. C), 139.38 (quart. C), 138.64 (quart. C), 138.46 (quart. C), 134.06 (quart. C), 133.94 (quart. C), 132.79 (CH–*C*), 132.08 (CH–*C*), 131.89 (CH–*D*), 130.77 (CH–*B*), 129.89 (quart. C), 129.52 (CH–*D*), 129.01 (quart. C), 127.73 (CH–*B*), 126.42 (quart. C), 121.28 (CH–*A*3), 66.24 (O–CH_3–*C*), 64.65 (O–CH_3–*D*), 62.20 (O–CH_3–*A*), 36.47 (quart. *t*Bu–C–*A*), 35.5, 34.8 and 34.8 (quart. *t*Bu–C–*B*,*C*,*D*), 30.76, 30.77 and 30.57 (quart. *t*Bu–C–*B*,*C*,*D*), 29.93 (*t*Bu–C–*A*).

X-ray measurements

Crystallographic data for 10a. M = 919.24 g mol^{-1}, monoclinic system, space group $P2_1/c$, a = 15.1655 (5) Å, b = 10.6137 (4) Å, c = 30.1233 (10) Å, β = 100.9433 (17)°, Z = 4, V = 4760.5 (3) Å^3, D_c = 1.282 g cm^{-3}, μ(Cu-Kα) = 2.32 mm^{-1}, crystal dimensions of 0.52 × 0.25 × 0.06 mm. Data were collected at 180 (2) K on a Bruker D8 Venture Photon CMOS diffractometer with Incoatec microfocus sealed tube Cu-Kα radiation. Data reduction, scaling and absorption correction were performed in Apex3.[21] The structure was solved by charge flipping methods[22] and anisotropically refined by full matrix least squares on F squared using CRYSTALS[23] to final value R = 0.048 and wR = 0.135 using 9046 independent reflections (θ_{max} = 70.5°), 749 parameters and 271 restraints. The hydrogen atoms bonded to carbon atoms were placed in calculated positions refined with riding constraints, while hydrogen atoms bonded to oxygen were refined using soft restraints, after which they were refined with riding constraints. The disordered functional group positions were found in different electron density maps and refined with restrained geometry. MCE[24] was used for the visualization of electron density maps. The occupancy of disordered functional groups was constrained to full. The structure has been deposited into the Cambridge Structural Database under number CCDC 2227440.†

Crystallographic data for 10b. M = 953.05 g mol^{-1}, triclinic system, space group $P\bar{1}$, a = 13.7722 (5) Å, b = 14.5337 (5) Å, c = 25.6391 (9) Å, α = 79.646 (2)°, β = 88.001 (2)°, γ = 78.359 (2)°, Z = 4, V = 4944.5 (3) Å^3, D_c = 1.280 g.cm^{-3}, μ(Cu-Kα) = 2.25 mm^{-1}, crystal dimensions of 0.42 × 0.27 × 0.07 mm. Data were collected at 180 (2) K on a Bruker D8 Venture Photon CMOS diffractometer with Incoatec microfocus sealed tube Cu-Kα radiation. Data reduction, scaling and absorption correction were performed in Apex4.[25] The structure was solved by charge flipping methods[22] and anisotropically refined by full matrix least squares on F squared using CRYSTALS[23] to final value R = 0.075 and wR = 0.191 using 18 737 independent reflections (θ_{max} = 70.4°), 1232 parameters and 66 restraints. The hydrogen atoms bonded to carbon atoms were placed in calculated positions refined with riding constraints, while hydrogen atoms bonded to oxygen were refined using soft restraints, after which they were refined using riding constraints. The disordered functional group positions were found in different electron density maps and refined with restrained geometry. MCE[24] was used for the visualization of electron density maps. The occupancy of disordered functional groups was constrained to full. The structure has been deposited into the Cambridge Structural Database under number CCDC 2227441.†

Crystallographic data for 10c. M = 1140.03 g mol^{-1}, triclinic system, space group $P\bar{1}$, a = 12.4947 (5) Å, b = 12.7653 (6) Å, c = 19.6418 (8) Å, α = 92.4959 (17)°, β = 90.0704 (16)°, γ = 112.6404 (15)°, Z = 2, V = 2888.1 (2) Å^3, D_c = 1.311 g cm^{-3}, μ(Mo-Kα) = 0.38 mm^{-1}, crystal dimensions of 0.53 × 0.34 × 0.23 mm. Data were collected at 180 (2) K on a Bruker D8 Venture Photon CMOS diffractometer with Incoatec microfocus sealed tube Mo-Kα radiation. Data reduction, scaling and absorption correction were performed in Apex4.[25] The structure was solved by charge flipping methods[22] and anisotropically refined by full matrix least squares on F squared using CRYSTALS[23] to the final value R = 0.057 and wR = 0.169 using 12 169 independent reflections (θ_{max} = 26.7°), 736 parameters and 89 restrains. The hydrogen atoms bonded to carbon atoms were placed in calculated positions refined with riding constraints, while hydrogen atoms bonded to oxygen were refined using soft restraints after which they were refined using riding constraints. The disordered functional group positions were found in different

electron density maps and refined with restrained geometry. MCE[24] was used for the visualization of electron density maps. The occupancy of disordered functional groups was constrained to full. The structure has been deposited into the Cambridge Structural Database under number CCDC 2227442.†

Crystallographic data for 11a. M = 889.14 g mol^{-1}, triclinic system, space group $P\bar{1}$, a = 14.1073 (2) Å, b = 17.6934 (5) Å, c = 19.5984 (4) Å, α = 70.921 (2)°, β = 89.7620 (14)°, γ = 83.5928 (17)°, Z = 4, V = 4591.58 (3) Å^3, D_c = 1.286 g cm^{-3}, μ(Cu-Kα) = 2.39 mm^{-1}, crystal dimensions of 0.42 × 0.29 × 0.07 mm. Data were collected at 95 (2) K on a Rigaku OD Supernova using an Atlas S2 CCD detector with Cu-Kα radiation from a microfocus sealed X-ray tube. Data reduction, scaling and absorption correction were performed in CrysAlis PRO.[26] The structure was solved by charge flipping methods[22] and anisotropically refined by full matrix least squares on F squared using CRYSTALS[23] to the final value R = 0.051 and wR = 0.136 using 18 212 independent reflections (θ_{max} = 74.6°), 1167 parameters and 116 restraints. The hydrogen atoms were placed in calculated positions refined with riding constraints. The disordered functional group positions were found in different electron density maps and refined with restrained geometry. MCE[24] was used for the visualization of electron density maps. The occupancy of disordered functional groups was constrained to full. Despite significant efforts, a suitable solvent disorder model could not be found; therefore, the solvent contribution to the structure factors was accounted for using PLATON squeeze,[27] resulting in a total solvent void volume of 374.6 Å^3. The structure has been deposited into the Cambridge Structural Database under number CCDC 2227443.†

Crystallographic data for 12a. M = 941.31 g mol^{-1}, monoclinic system, space group $P2_1/a$, a = 11.7275 (7) Å, b = 35.321 (2) Å, c = 12.2803 (6) Å, β = 101.3240 (19)°, Z = 4, V = 4987.7 (5) Å^3, D_c = 1.253 g cm^{-3}, μ(Mo-Kα) = 0.25 mm^{-1}, crystal dimensions of 0.42 × 0.24 × 0.17 mm. Data were collected at 293 (2) K on a Bruker D8 Venture Photon CMOS diffractometer with Incoatec microfocus sealed tube Mo-Kα radiation. The data reduction, scaling and absorption correction were performed in Apex3.[21] The structure was solved by charge flipping methods[22] and anisotropically refined by full matrix least squares on F squared using CRYSTALS[23] to final value R = 0.041 and wR = 0.104 using 10 265 independent reflections (θ_{max} = 26.4°), 710 parameters and 255 restraints. The hydrogen atoms were placed in calculated positions refined with riding constraints. The disordered functional group positions were found in different electron density maps and refined with restrained geometry. MCE[24] was used for the visualization of electron density maps. The occupancy of disordered functional groups was constrained to full. The structure has been deposited into Cambridge Structural Database under number CCDC 2227444.†

Calculations

The conformational screening was performed in CREST version 2.11,[28] using default settings. The DFT geometry optimizations were performed in ORCA 5.0.3,[29] using B3LYP[30] functional with a def2-SVP basis set[31] employing the RIJCOSX approximation,[32] with a def2/J auxiliary basis set[33] and D3BJ corrections.[34]

Final single point energies were obtained at DLPNO-CCSD (T) with a def2-QZVPP[31] basis set, def2/J auxiliary basis set[33] and def-QZVPP/C auxiliary basis set for CC,[35] using the RIJCOSX approximation.[32]

Geometries of the most favourable isomers of all stationary points at the DFT level are reported in the ESI.†

Conflicts of interest

There are no conflicts to declare.

Acknowledgements

This research was supported by the Czech Science Foundation (Grant 20-08667S).

References

1 H. Kumagai, M. Hasegawa, S. Miyanari, Y. Sugawa, Y. Sato, T. Hori, S. Ueda, H. Kamiyama and S. Miyano, *Tetrahedron Lett.*, 1997, **38**, 3971.

2 For selected books on calixarenes and their applications, see: (*a*) *Calixarenes and Beyond*, ed. P. Neri, J. L. Sessler and M. X. Wang, Springer, Cham, Switzerland, 2016; (*b*) C. D. Gutsche, *Calixarenes: An Introduction*, Royal Society of Chemistry, Cambridge, U.K., 2nd edn, 2008; (*c*) *Calixarenes in the Nanoworld*, ed. J. Vicens, J. Harrowfield and L. Backlouti, Springer, Dordrecht, The Netherlands, 2007; (*d*) *Calixarenes 2001*, ed. Z. Asfari, V. Böhmer, J. Harrowfield and J. Vicens, Kluwer, Dordrecht, The Netherlands, 2001; (*e*) *Calixarenes in Action*, ed. L. Mandolini and R. Ungaro, Imperial College Press, London, 2000.

3 For recent reviews on thiacalixarenes, see: (*a*) R. Kumar, Y. O. Lee, V. Bhalla, M. Kumar and J. S. Kim, *Chem. Soc. Rev.*, 2014, **43**, 4824; (*b*) N. Morohashi, F. Narumi, N. Iki, T. Hattori and S. Miyano, *Chem. Rev.*, 2006, **106**, 5291; (*c*) P. Lhotak, *Eur. J. Org. Chem.*, 2004, 1675.

4 (*a*) A. M. Litwak and S. E. Biali, *J. Org. Chem.*, 1992, **57**, 1945; (*b*) S. E. Biali, *Synlett*, 2003, 1; (*c*) A. M. Litwak, F. Grynszpan, O. Aleksiuk, S. Cohen and S. E. Biali, *J. Org. Chem.*, 1993, **58**, 393.

5 For selected examples of a spirodienone route to the derivatization of classical calixarenes, see: (*a*) C. Gaeta, F. Troisi, C. Talotta, T. Pierro and P. Neri, *J. Org. Chem.*, 2012, **77**, 3634; (*b*) F. Troisi, T. Pierro, C. Gaeta and P. Neri, *Tetrahedron Lett.*, 2009, **50**, 4416; (*c*) S. Simaan and S. E. Biali, *J. Org. Chem.*, 2004, **69**, 95; (*d*) S. Simaan, K. Agbaria and S. E. Biali, *J. Org. Chem.*, 2002, **67**, 6136; (*e*) K. Agbaria and S. E. Biali, *J. Am. Chem. Soc.*, 2001, **123**,

12495; (*f*) K. Agbaria, J. Wöhnert and S. E. Biali, *J. Org. Chem.*, 2001, **66**, 7059.

6 N. Morohashi, M. Kojima, A. Suzuki and Y. Ohba, *Heterocycl. Commun.*, 2005, **11**, 249.

7 (*a*) K. Polivkova, M. Simanova, J. Budka, P. Curinova, I. Cisarova and P. Lhotak, *Tetrahedron Lett.*, 2009, **50**, 6347; (*b*) L. Vrzal, M. Kratochvilova-Simanova, T. Landovsky, K. Polivkova, J. Budka, H. Dvorakova and P. Lhotak, *Org. Biomol. Chem.*, 2015, **13**, 9610.

8 (*a*) T. Landovsky, H. Dvorakova, V. Eigner, M. Babor, M. Krupicka, M. Kohout and P. Lhotak, *New J. Chem.*, 2018, **42**, 20074–20086; (*b*) T. Landovsky, M. Tichotova, L. Vrzal, J. Budka, V. Eigner, H. Dvorakova and P. Lhotak, *Tetrahedron*, 2018, **74**, 902–907.

9 (*a*) K. Flidrova, P. Slavik, V. Eigner, H. Dvorakova and P. Lhotak, *Chem. Commun.*, 2013, **49**, 6749; (*b*) P. Slavik, V. Eigner and P. Lhotak, *CrystEngComm*, 2016, **18**, 4964.

10 (*a*) P. Slavik, H. Dvorakova, M. Krupicka and P. Lhotak, *Org. Biomol. Chem.*, 2018, **16**, 838; (*b*) P. Slavik, M. Krupicka, V. Eigner, L. Vrzal, H. Dvorakova and P. Lhotak, *J. Org. Chem.*, 2019, **84**, 4229.

11 T. Landovsky, V. Eigner, M. Babor, M. Tichotova, H. Dvorakova and P. Lhotak, *Chem. Commun.*, 2020, **56**, 78–81.

12 T. Landovsky, M. Babor, J. Cejka, V. Eigner, H. Dvorakova, M. Krupicka and P. Lhotak, *Org. Biomol. Chem.*, 2021, **19**, 8075–8085.

13 J. Miksatko, V. Eigner, H. Dvorakova and P. Lhotak, *Tetrahedron Lett.*, 2016, **57**, 3781–3784.

14 Similar observations regarding *exo*- and *endo*- stereoisomers of calixarenes and an *exo*/*endo* attack with respect to the calixarene cavity were also discussed in: F. Troisi, T. Pierro, C. Gaeta and P. Neri, *Org. Lett.*, 2009, **11**, 697–700.

15 For selected example papers on photochemical stereomutation of the sulfoxide group, see: (*a*) K. Mislow, M. Axelrod, D. R. Rayner, H. Gotthardt, L. M. Coyne and G. S. Hammond, *J. Am. Chem. Soc.*, 1965, **87**, 4958–4959; (*b*) W. S. Jenks, D. D. Gregory, Y. Guo, W. Lee and T. Tetzlaff, *Mol. Supramol. Photochem.*, 1997, **1**, 1–56; (*c*) W. S. Jenks, W. Lee and D. Shutters, *J. Phys. Chem.*, 1994, **98**, 2282–2289; (*d*) W. Lee and W. S. Jenks, *J. Org. Chem.*, 2001, **66**, 474–480.

16 This is in contrast to the only paper devoted to the photoisomerization of the sulfoxide group in thiacalix[4]arenes, where the authors successfully used 283 nm light. On the other hand, they used much shorter reaction times (4 min), see: R. Cacciapaglia, S. Di Stefano, O. Lanzalunga, L. Maugeri and M. Mazzonna, *Eur. J. Org. Chem.*, 2012, 1426–1430.

17 (*a*) A. Bondi, *J. Phys. Chem.*, 1964, **68**, 441–451; (*b*) R. S. Rowland and R. Taylor, *J. Phys. Chem.*, 1996, **100**, 7384–7391; (*c*) M. Mantina, A. C. Chamberlin, R. Valero, C. J. Cramer and D. G. Truhlar, *J. Phys. Chem. A*, 2009, **113**, 5806–5812.

18 (*a*) L. Vogel, P. Wonner and S. M. Huber, *Angew. Chem., Int. Ed.*, 2019, **58**, 1880–1891; (*b*) D. J. Pascoe, K. B. Ling and S. L. Cockroft, *J. Am. Chem. Soc.*, 2017, **139**, 15160–15167; (*c*) W. Wang, B. Ji and Y. Zhang, *J. Phys. Chem. A*, 2009, **113**, 8132–8135; (*d*) K. T. Mahmudov, M. N. Kopylovich, M. F. C. Guedes da Silva and A. J. L. Pombeiro, *Dalton Trans.*, 2017, **46**, 10121–10138.

19 For examples of deoxygenation of sulfoxides, see: (*a*) J. Drabowicz, T. Numata and S. Oae, *Org. Prep. Proced. Int.*, 1977, **9**, 63–83; (*b*) G. M. Gurria and G. H. Posner, *J. Org. Chem.*, 1973, **38**, 2419–2420; (*c*) L. Shiri and M. Kazemi, *Res. Chem. Intermed.*, 2017, **43**, 6007–6041.

20 For the nature of highly reactive oxygen species formed, see: (*a*) D. D. Gregory, Z. Wan and W. S. Jenks, *J. Am. Chem. Soc.*, 1997, **119**, 94–102; (*b*) Z. Wan and W. S. Jenks, *J. Am. Chem. Soc.*, 1995, **117**, 2667–2668.

21 Bruker, *APEX3, SAINT*, Bruker AXS Inc., Madison, Wisconsin, USA, 2015.

22 L. Palatinus and G. Chapuis, *J. Appl. Crystallogr.*, 2007, **40**, 786–790.

23 P. W. Betteridge, J. R. Carruthers, R. I. Cooper, K. Prout and D. J. Watkin, *J. Appl. Crystallogr.*, 2003, **36**, 1487.

24 J. Rohlicek and M. Husak, *J. Appl. Crystallogr.*, 2007, **40**, 600.

25 Bruker, *APEX4, SAINT and SADABS*, Bruker AXS Inc., Madison, Wisconsin, USA, 2021.

26 Rigaku OD, *CrysAlis PRO*, Rigaku Oxford Diffraction Ltd, Yarnton, Oxfordshire, England, 2020.

27 A. L. Spek, *Acta Crystallogr., Sect. C: Struct. Chem.*, 2015, **71**, 9–18.

28 P. Pracht, F. Bohle and S. Grimme, *Phys. Chem. Chem. Phys.*, 2020, **22**, 7169–7192.

29 F. Neese, *Wiley Interdiscip. Rev.: Comput. Mol. Sci.*, 2012, **2**, 73–78.

30 A. D. Becke, *J. Chem. Phys.*, 1993, **98**, 5648–5652.

31 F. Weigend and R. Ahlrichs, *Phys. Chem. Chem. Phys.*, 2005, **7**, 3297–3305.

32 F. Neese, F. Wennmohs, A. Hansen and U. Becker, *Chem. Phys.*, 2009, **356**, 98–109.

33 F. Weigend, *Phys. Chem. Chem. Phys.*, 2006, **8**, 1057–1065.

34 (*a*) S. Grimme, J. Antony, S. Ehrlich and H. Krieg, *J. Chem. Phys.*, 2010, **132**, 154104; (*b*) S. Grimme, S. Ehrlich and L. Goerigk, *J. Comput. Chem.*, 2011, **32**, 1456–1465.

35 A. Hellweg, C. Hättig, S. Höfener and W. Klopper, *Theor. Chem. Acc.*, 2007, **117**(4), 587–597.

